Thin Solid Films 520 (2011) 1048–1052

Contents lists available at SciVerse ScienceDirect

Thin Solid Films

journal homepage: www.elsevier.com/locate/tsf

Aerosol based fabrication of a Cu/polymer and its application for electromagnetic interference shielding

Jeong Hoon Byeon [a], Jang-Woo Kim [b,*]

[a] Department of Chemistry, Purdue University, IN 47907, United States
[b] Department of Digital Display Engineering, Hoseo University, Asan 336-795, Republic of Korea

ARTICLE INFO

Article history:
Received 26 May 2011
Received in revised form 15 August 2011
Accepted 16 August 2011
Available online 23 August 2011

Keywords:
Surface activation
Electromagnetic interference shielding
Copper
Polymer substrates
Paladium
Nanoparticles
Electroless deposition

ABSTRACT

The effect of a catalytic surface activation on the electromagnetic interference shielding of Cu deposited polymer substrates was investigated. The surface of polymer substrates was catalytically activated by different methods respectively adopted Pd aerosol nanoparticles and Sn–Pd wet chemical processes. Although both activations initiated the deposition of Cu on the substrates, differences such as morphology (Pd aerosol: ~80 nm vs Sn–Pd: ~140 nm, in Cu grain size) and composition (Pd aerosol: Cu and Pd *vs* Sn–Pd: Cu, Pd, Sn, and Cl) of Cu deposits were presented. Specimens activated using Pd aerosol nanoparticles showed a higher range of shielding effectiveness by about 4–10 dB than those activated by Sn–Pd processes in 2–18 Ghz frequencies.

1. Introduction

A variety of composites (i.e. metal layer on polymer) have been used for either decorative or functional purposes in applications such as food packaging, microelectronics packaging, and coatings for electromagnetic interference (EMI) shielding and wear protection [1–4]. In particular, to have a better degree of EMI shielding effectiveness, metal deposition techniques have been suggested and commercially produced [5,6] since metal deposits could reflect or conduct the free electrons [7]. The most widely used metals are Al, Cu, Ag, and Ni [8]. Polymer substrates have many advantages, such as portability, low cost, easy construction of complex shapes, superior design capabilities, etc. [3]. For depositing metal on substrates, electroless deposition (ELD) has strong advantages over sputtering, chemical vapor deposition, and electrodeposition, particularly with respect to its cost performance, the use of nonconductive substrates with complex shapes, and simple equipment [9–13]. A number of research papers have taken into account the kinetics of metal ELD on the various substrates, determining the deposition rate as a function of various solution components and conditions. However, the deposition is initiated upon the catalytically activated surface, and the deposition reaction is sustained by the catalytic nature of the deposited metal surface itself, so that properties of the electroless deposited metals are highly dependent on the activation method.

The initiation of the ELD process is preceded by surface activation to provide ELD initiation sites (i.e. initiators) on the substrate's surface [14]. The initiator is an electron carrier in the transfer of electrons from the reducer to metal ions in the ELD bath [15]. It is usually carried out in solutions of Sn sensitization and Pd activation, i.e. Sn–Pd activation. Since Sn sensitization makes the layer inactive toward ELD, this layer should be removed in the following acceleration step, and therefore, continued study on activation methods is needed to improve ELD and to reduce the usage of environmentally toxic agents. Concerning this problem, an activation method using Pd aerosol nanoparticles was introduced which involves fewer steps than the Sn–Pd activation and less contains unwanted impurities [16].

In this paper, we present a method using Cu on a polymer substrate (polytetrafluoroethylene, PTFE), Cu/polymer, as an EMI shielding material, fabricated by an ELD using Pd aerosol nanoparticles produced by an ambient spark discharge to apply EMI shielding effectiveness. Recently, the replacement of the activation method of the substrate is an area of interest for improving the EMI shielding effectiveness of a Cu/polymer substrate [5,17,18]. However, the effect of the activation method is still limited only to wet chemical activation or vacuum plasma treatment processes for EMI shielding applications and therefore there is not much information available concerning the appropriate fabrication process.

* Corresponding author. Tel.: +82 41 540 5925; fax: +82 41 540 5929.
E-mail address: jwkim@hoseo.edu (J.-W. Kim).

0040-6090/$ – see front matter
doi:10.1016/j.tsf.2011.08.064

2. Experimental details

Fig. 1 shows a diagram of the method used to a fabricate Cu/polymer. A spark discharge was used to produce Pd aerosol nanoparticles under ambient conditions as initiators for an ELD [16,19,20], and the particles were captured by the 'untreated' polymer substrate (11807-47-N, Sartorius) by a physical filtration. The PTFE substrate was selected because of its superior chemical resistance (hydrophobicity), good thermal stability, and high mechanical strength [21]. After annealing at 240 °C, the initiator fixed, so-called 'activated,' substrate was immersed horizontally in a Cu ELD. An applying temperature for the annealing was concerned with a critical temperature of thermal deformation or cracks of substrate (i.e. the melting temperature of PTFE = 327 °C).

For comparison purposes, the surface of another substrate was activated by a Sn–Pd process (also in Fig. 1), which requires Sn sensitization. The substrate was first sensitized by immersing it in an aqueous solution containing $SnCl_2$ (8 mg), HCl (0.05 mL), and deionized (DI) water (49.95 mL), followed by rinsing with DI water. The activated substrate was accelerated by immersing it in an aqueous solution containing NaOH (1 g) and DI water (50 mL) to remove Sn species over the catalytic Pd particles, followed by rinsing with DI water. The subsequent activation was carried out in a $PdCl_2$ solution of $PdCl_2$ (4 mg), HCl (0.05 mL), and DI water (49.95 mL), followed by rinsing again with DI water.

Solution A contained 5 g of $CuSO_4$, 30 g of $KNaC_4H_4O_6\,4H_2O$ (Rochelle salt) and 6 g of NaOH in 100 ml of DI water. Solution B was an aqueous HCHO solution (37.2 wt.%). Solutions A and B were mixed at a 10:1 (v/v) ratio and the activated substrate was immersed into the mixture. Herein, the filtered Pd nanoparticles acted as a catalyst for the subsequent Cu deposition in the ELD bath. It is known that the ELD process is electrochemical in nature [22]. The beginning of the ELD is controlled by the anodic processes. Under the catalytic action of Pd nanoparticles fixed on the substrate surface, Cu^{2+} ions are deposited onto the catalytic Pd surface by the capturing electrons that are furnished by the HCHO via the following reactions [23]:

$$\text{anodic reaction: } HCHO + 2OH^- \xrightarrow{Pd} HCOO^- + H_2O + 2H^{\cdot} + 2e \rightarrow H_2\uparrow \quad (1)$$

$$\text{cathodic reaction : } Cu^{2+} + 2e \rightarrow Cu\downarrow \quad (2)$$

In aqueous solutions, the HCHO which is adsorbed on the catalytic Pd surfaces is easily oxidized to yield $HCOO^-$, the activated hydrogen atom ($H^{\cdot}$) and released electrons (e), while Cu^{2+} in the ELD bath are reduced to metallic Cu by the electrons generated through the oxidation of HCHO. Once the Cu deposition was initiated, the deposited Cu themselves acted as self-catalysts for further Cu deposition.

Field-emission scanning electron microscope (SEM, JSM-6500F, JEOL) images and energy dispersive X-ray (EDX, JED-2300, JEOL) profiles were obtained at an accelerating voltage of 15 kV. Atomic force microscope (AFM) was consisted of an E scanner (NanoScope IIIa) having a maximum scanning size of 125 μm and a resolution of 0.02 nm. The drive frequency was 330 kHz, and the voltage was between 3.0 and 4.0 V. The drive amplitude was about 300 mV, and the scan rate was 0.5–1.0 Hz. X-ray diffraction (XRD) studies of the fabricated samples were carried out on a Rigaku RINT-2100 diffractometer equipped with a thin-film attachment using Cu-Kα radiation (40 kV, 40 mA). The 2θ angles ranged from 10 to 90° at $4°\,min^{-1}$ by step scanning at an interval of 0.08°.

The EMI shielding effectiveness of the fabricated samples (also in Fig. 1) was tested by the Electro-Metrics Model EM-2107 shielding effectiveness test fixture according to ASTM D 4935-89. For calibration, the signal generator and receiver were set at the same frequency check point and recorded electric power values. The EMI shielding effectiveness was determined for the frequency points selected with repetition. The shielding effectiveness value (E_s) expressed in decibels (dB) was calculated from the ratio of the incident to the transmitted power of the electromagnetic wave in the following equation [10,24]:

$$E_s = 10\,log\left|\frac{P_i}{P_a}\right| = 20\,log\left|\frac{E_i}{E_a}\right| = 20\,log\left|\frac{H_i}{H_a}\right| \quad (3)$$

where P_a, E_a, and H_a are the energy field strength, electric field strength, and magnetic field strength, respectively, of the transmitted wave, and P_i, E_i, and H_i are the above properties of the incident wave.

All experiments and measurements were performed four times and the following data described with averaged values.

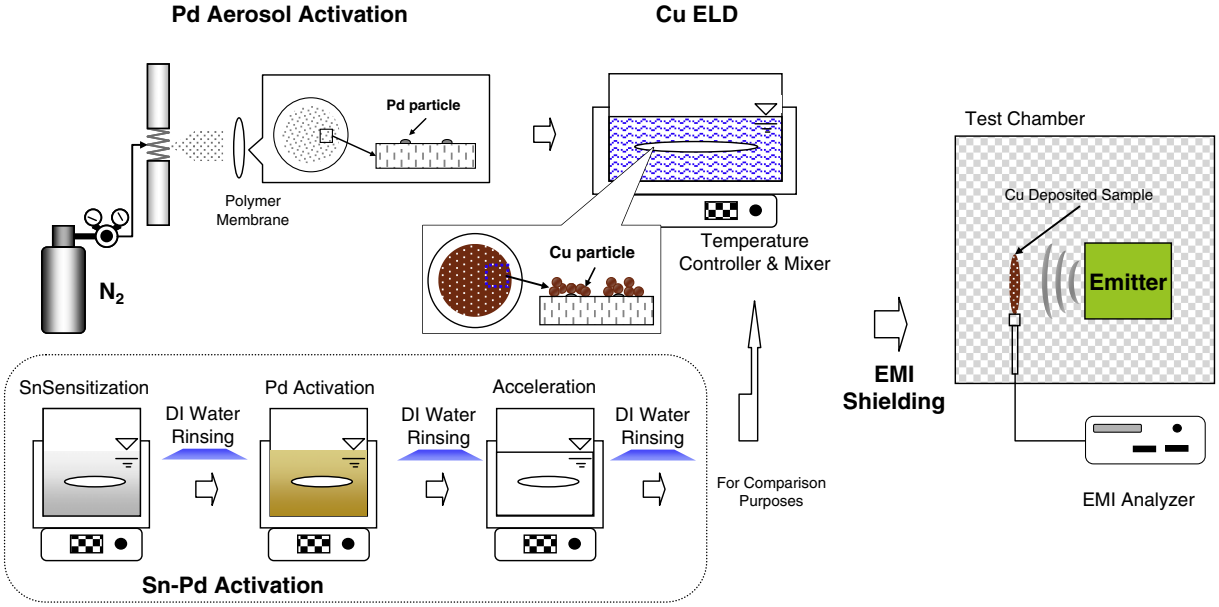

Fig. 1. Diagram of fabrication procedures and the procedure for testing the EMI shielding qualities.

3. Results and discussion

The SEM images (Fig. 2a) show that the untreated substrate had a clean surface, while a number of particles were presented on the activated substrates. The mean mode diameter of the single (or primary) aerosol particles was approximately 4 nm; this fact had been proven by transmission electron microscopy in the earlier report [25]. From EDX spectroscopic analyses (Fig. 2b), it was found that the untreated substrate contained C and F, which might have originated from the substrate, while the activated substrates contained a small amount of Pd. The conventionally activated substrate also contained a small amount of Sn and Cl, which might have originated from Sn sensitization. From the above characterizations, an activation intensity (I_a) of substrate with Pd aerosol nanoparticles is defined as follows [25]:

$$I_a = Q \cdot t_a \cdot A_m^{-1} \int_0^{\infty} \eta\left(D_p\right) C_a\left(D_p\right) dD_p \tag{4}$$

where, Q is the flow rate of carrier gas, t_a is the activation time, A_m is the plane area of membrane, and C_a (D_p) is the area concentration of Pd particles (measured by a scanning mobility particle sizer, 3936, TSI). The activation intensity was selected to be approximately 6.2 cm^2 of Pd cm^{-2} of substrate (or 50 μg of Pd cm^{-2} of substrate). For comparison purposes, the activation intensity was chosen to be 50 μg of Pd cm^{-2} of substrate from Sn–Pd processes, which was same as that for the aerosol activation and achieved by a trial-error method using an inductively coupled plasma atomic emission spectroscope (ICPAES, Elan 6000, Perkin-Elmer). A SEM image for the Sn–Pd activated substrate is also displayed in Fig. 2a, and a uniformity of spot distribution was rather poor compared to that for aerosol activation.

The morphology of Cu deposits activated with the different methods was examined by SEM. Fig. 3a represents the SEM images with different magnifications of the structure of the Cu deposit having an amount of 1.03 mg of Cu cm^{-2} of substrate from both activations. The Cu deposit from the Pd aerosol activation is comprised smaller particle (~80 nm in grain size) aggregates, but unevenly distributed bigger particle (~140 nm in grain size) aggregates were found in the Cu deposit from Sn–Pd activation. This might represent a sensitive diagnosis of the availability of the initiator and how uniform it was on the surface (refer Fig. 2a). Only when the surface was uniformly covered with Pd particles, could a dense and uniform Cu deposit be obtained. A report from Tong et al. [26] indeed described that the uniformity of the metal deposit was largely influenced by the dispersion of initiator particles, and the nucleation resulted in particles formed directly on the top of the initiator layer [26]. Otherwise, with the influence of the hydrogen release at the surface (refer Eq. (1)), some neighboring Cu particles tended to aggregate along the gas bubble and grew in three dimensions. Since Pd particles were located in different areas of the substrate surface (refer Fig. 2a), the probability of Cu particle formation on different Pd particles during ELD was expected to be different, i.e. a shadowing effect. Due to an initial microstructural non-uniformity, some particles could grow faster than others, leading to non-uniformity of the formed deposit microstructure. Thereby, packets with dense chain-network particles were formed on the substrates.

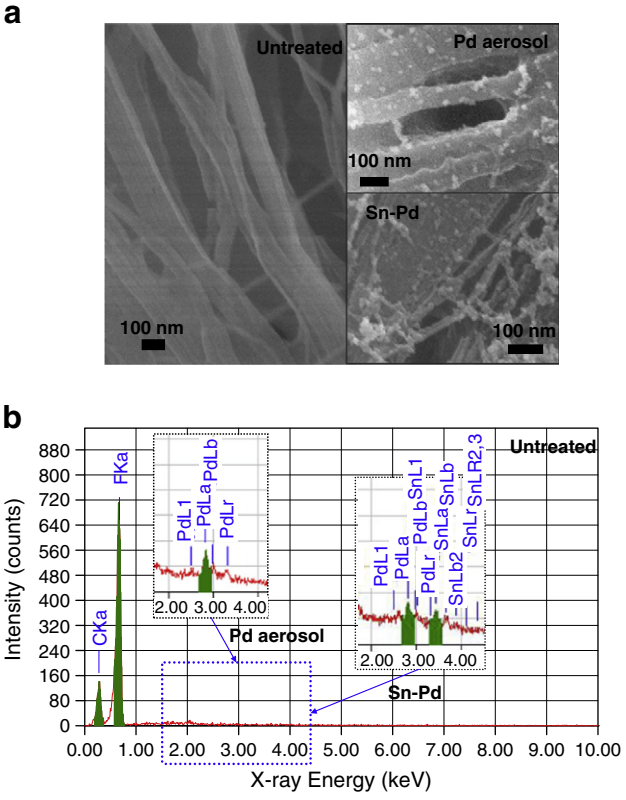

Fig. 2. (a) SEM images of untreated and activated (Pd aerosol and Sn–Pd) surfaces of polymer substrates. (b) EDX profiles of the untreated and activated substrates.

The images in Fig. 3b show EDX maps of the SEM images displayed in Fig. 3a. These maps for the aerosol activation corresponded to Pd and Cu while Sn and Cl dots were also contained for the Sn–Pd activation. The dots in these images indicated the positions of each element in the SEM images. For example, Cu dots were prominently presented in the area corresponding to the white deposits in the SEM images. Details of the compositions were described in Table 1.

Fig. 3c shows a flattened AFM image of Cu deposit topographs (having an amount of 1.03 mg of Cu cm^{-2} of substrate) obtained in the tapping mode. The thickness and arithmetic mean roughness of the deposits from the aerosol activation (or Sn–Pd activation) were approximately 3.2 (3.1) μm and 51.4 (113.1) nm, respectively. A difference of the estimated dimensional growth rates between the activations were slight but the surface roughness of the deposits showed a quite difference owing to different activation results (refer Fig. 2a).

Fig. 3d shows the XRD patterns of Cu deposited samples from both activations (having an amount of 1.03 mg of Cu cm^{-2} of substrate). The four major characteristic peaks of the samples at $2\theta = 43.4$, 50.6, 74.3, and 90.2° corresponded to the crystal faces of (111), (200), (220), and (311) of Cu, respectively, implying that the Cu deposits had a conductive property. According to the Scherrer equation, the average size of the Cu particles from the Pd aerosol and Sn–Pd activations were respectively 31.7 and 47.1 nm with respect to the Cu (111) main peaks. The Cu deposit from the aerosol activation comprised finer particles than that from the Sn–Pd activation. From the SEM and XRD results, the Cu particles for the Pd aerosol and Sn–Pd activations were mainly consisted of Cu crystals with sizes of about 30 and 50 nm, respectively.

Fig. 4 indicates the shielding effectiveness of the Cu/polymer samples from the Pd aerosol and Sn–Pd activations. The shielding effectiveness of the Cu/polymer samples stayed at a similar level at the frequency range of 2–18 GHz. Specimens activated using Pd aerosol nanoparticles showed a higher range of shielding effectiveness by about 4–10 dB compared to those activated using the Sn–Pd processes in the frequencies. It was a possibility that the effectiveness loss of the deposit from the Sn–Pd activation was caused by a relatively lower purity (corresponding conductance), resulting in a substantial lower effectiveness. Indeed, when the Sn–Pd activation was performed, impurities such as Sn (2.8–1.6% by mass) and Cl (0.7–0.2% of the total number of atoms) compounds remained. Moreover, the morphological difference (refer Fig. 3a) of the deposits from the different activations also affected the discrepancies; longer Cu particle chains were dispersed on the substrate from the Pd aerosol activation, which

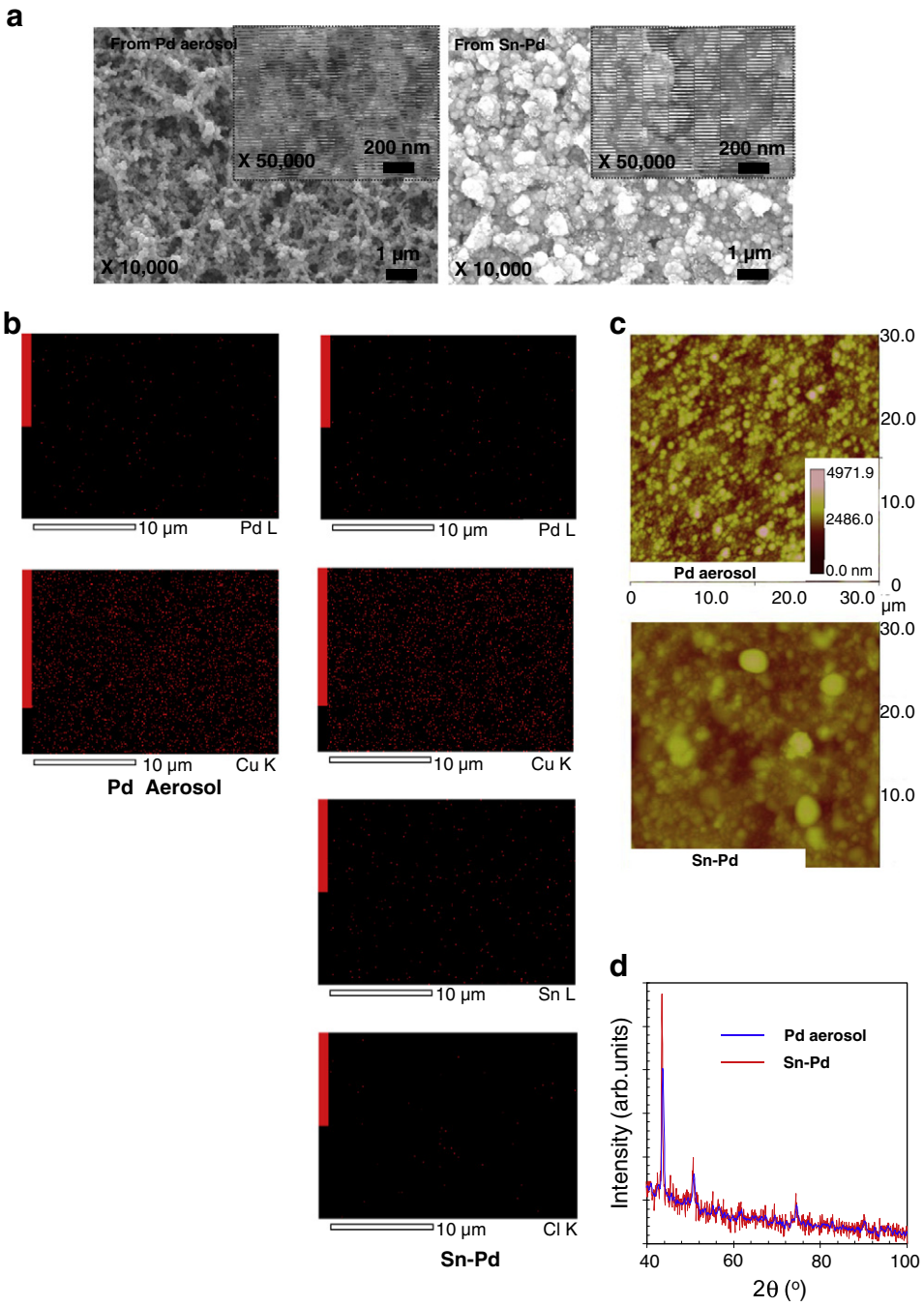

Fig. 3. (a) SEM images of Cu/polymer samples (30 min ELD) from Pd aerosol and Sn–Pd activations. (b) EDX maps of the Cu/polymer samples. (c) Topographs of the Cu deposits from Pd aerosol and Sn–Pd activations. (d) XRD results of the Cu deposits from Pd aerosol and Sn–Pd activations.

can probably be attributed to the percolation phenomenon. Nevertheless, as the ELD time increased, there were no remarkable differences in the effectiveness between the activations. A relatively smaller difference of the composition ratio (refer to R in Table 1) between the surface activation and the Cu deposition probably caused the decline of the difference.

4. Conclusions

The surface of PTFE substrates were catalytically activated by different methods respectively adopted Pd aerosol nanoparticles and Sn–Pd wet chemical processes. Although both activations initiated the deposition of Cu on the substrates, differences such as morphology

Table 1
Elemental composition of Cu deposited polymer substrates.

Element (mass %)	Pd aerosol			Sn–Pd		
	ELD time (min)					
	10	20	30	10	20	30
C	43.5	30.1	22.9	42.9	29.6	22.2
F	12.5	9.4	7.5	11.9	8.8	7.2
Pd	2.1	1.4	1.1	1.9	1.0	0.9
Cu	41.9	59.1	68.5	39.8	58.4	67.9
Sn	–	–	–	2.8	1.9	1.6
Cl	–	–	–	0.7	0.3	0.2
R	Pd / Cu	Pd + Sn + Cl / Cu				
	0.050	0.024	0.016	0.136	0.055	0.039

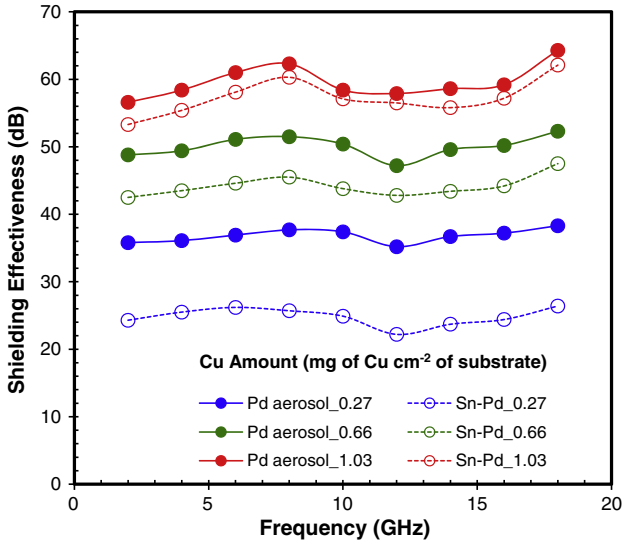

Fig. 4. Shielding effectiveness of Cu/polymer samples from Pd aerosol and Sn–Pd activations.

(Pd aerosol: ~80 nm vs Sn–Pd: ~140 nm, in Cu grain size) and composition (Pd aerosol: Cu and Pd *vs* Sn–Pd: Cu, Pd, Sn, and Cl) of Cu deposits were presented. Specimens activated using Pd aerosol nanoparticles showed a higher range of shielding effectiveness by about 4–10 dB than those activated by Sn–Pd processes in 2–18 Ghz frequencies, which might have originated from the activation characteristics of the Pd aerosol (pure Pd with uniform dispersion) and Sn–Pd (Pd, Sn, etc., with non-uniform dispersion) methods. This strategy may be attractive for various scientific and/or engineering applications for EMI shielding including catalytic electrodes, catalysts, and etc., because the aerosol activation of the substrate is simple, environmentally friendly, and effective (with less impurity).

References

[1] X. Gan, Y. Wu, L. Liu, B. Shen, W. Hu, Surf. Coat. Technol. 201 (2007) 7018.
[2] L.T. Romankiw, Electrochim. Acta 42 (1997) 2985.
[3] C.-Y. Huang, W.-W. Mo, M.-L. Roan, Surf. Coat. Technol. 184 (2004) 123.
[4] Y. Lu, S. Jiang, Y. Huang, Surf. Coat. Technol. 204 (2010) 2829.
[5] E.G. Han, E.A. Kim, K.W. Oh, Synth. Met. 123 (2001) 469.
[6] K.W. Oh, D.J. Kim, S.H. Kim, J. Appl. Polym. Sci. 84 (2002) 1369.
[7] S. Geetha, K.K.S. Kumar, C.R.K. Rao, M. Vijayan, D.C. Trivedi, J. Appl. Polym. Sci. 112 (2009) 2073.
[8] J.H. Moon, K.H. Kim, H.W. Choi, S.W. Lee, S.J. Park, Ultramicroscopy 108 (2008) 1307.
[9] C.-C. Chen, C.-W. Hung, S.-Y. Yang, C.-Y. Huang, J. Appl. Polym. Sci. 109 (2008) 3679.
[10] T. Bhuvana, G.V.P. Kumar, G.U. Kulkarni, C. Narayana, J. Phys. Chem. C 111 (2007) 6700.
[11] R.H. Guo, S.Q. Jiang, C.W.M. Yuen, M.C.F. Ng, J. Appl. Electrochem. 39 (2009) 907.
[12] C. Chujiang, Y. Xiaozheng, S. Zhigang, X. Yushan, J. Phys. D: Appl. Phys. 40 (2007) 6026.
[13] Y.-J. Hu, H.-Y. Zhang, F. Li, X.-L. Cheng, T.-L. Chen, Polym. Test. 29 (2010) 609.
[14] Y.-H. Chen, C.-Y. Huang, F.-D. Lai, M.-L. Roan, K.-N. Chen, J.-T. Yeh, Thin Solid Films 517 (2009) 4984.
[15] L.-C. Kuo, Y.-C. Huang, C.-L. Lee, Y.-W. Yen, Electrochim. Acta 52 (2006) 353.
[16] J.H. Byeon, J. Hwang, ACS Appl. Mater. Interfaces 1 (2009) 261.
[17] R.H. Guo, S.Q. Jiang, C.W.M. Yuen, M.C.F. Ng, J. Mater. Sci. Mater. Electron. 20 (2009) 33.
[18] M. Štefečka, M. Kando, H. Matsuo, Y. Nakashima, M. Koyanagi, T. Kamiya, M. Černák, J. Mater. Sci. 39 (2004) 2215.
[19] J.H. Byeon, K.Y. Yoon, J. Hwang, Thin Solid Films 518 (2010) 6839.
[20] J.H. Byeon, J.-W. Kim, Thin Solid Films 519 (2010) 700.
[21] Y.-L. Liu, C.-H. Yu, J.-Y. Lai, J. Membr. Sci. 315 (2008) 106.
[22] H. Dai, H. Li, F. Wang, Surf. Coat. Technol. 201 (2006) 2859.
[23] S. Shukla, S. Seal, J. Akesson, R. Oder, R. Carter, Z. Rahman, Appl. Surf. Sci. 181 (2001) 35.
[24] W. Zeng, S.T. Tan, Polym. Compos. 27 (2006) 24.
[25] J.H. Byeon, B.J. Ko, J. Hwang, J. Phys. Chem. C 112 (2008) 3627.
[26] H. Tong, L. Zhu, M. Li, C. Wang, Electrochim. Acta 48 (2003) 2473.